A Proliferation Assessment of Third Generation Laser Uranium Enrichment Technology

Ryan Snyder

Program on Science and Global Security
Princeton University
Princeton, NJ, USA

Section A: Possible Lasers for Third Generation Laser Enrichment

For any laser to be usable with third generation laser enrichment technology, it must emit light at either 16 or 5.3 μm. There are other performance characteristics, however, that must be considered when assessing the effectiveness some laser systems, and how accessible certain modifications to these systems may be to make them usable. These include the laser's pulse repetition rate, the linewidth of the emitted pulses, how easily the central peak of the emitted pulse may be tuned to the desired wavelength, the duration of the pulse, and the energy fluence in each pulse. While there may be certain challenges with different systems in achieving what is considered ideal for uranium enrichment, some level of enrichment is still possible even if not all ideal performance characteristics are met, and cascading to 90 percent HEU may still be desirable if either obtaining more lasers, spending more money, using more space, or taking more time is possible and tolerable for the proliferator.

Raman-shifted Transversely-Excited Atmospheric (TEA) CO_2 Laser at 16 μm

It is widely speculated that a Raman-shifted TEA CO_2 laser is to be employed with SILEX. Such lasers operate by applying a pulsed RF discharge transversely across the resonator tube containing CO_2 gas at a pressure of at least 1 atm, but it is more likely that a higher pressure ($\sim 5-8$ atm) is necessary for successful SILEX operation. What is necessary to understand, however, is the equipment and performance characteristics needed to generate pulses of ~ 10 mJ (see section "Laser performance characteristics" in the main section of the paper) that allow for high selectivity (narrow laser linewidth) at the precisely tuned wavelength: 15.916 μm for the ν_3 mode of $^{235}UF_6$ and only slightly different at 15.931 μm for $^{238}UF_6$. Given that the vibrational and rotational modes of a CO_2 molecule emit light between $9-11$ μm, CO_2 laser light must be down-shifted to the $^{235}UF_6$ ν_3 line by Raman scattering.

Raman Scattering

Raman scattering is defined as the inelastic scattering of photons, and therefore involves either giving up (Stokes wave) or acquiring more (anti-Stokes wave) energy. For SILEX, a Stokes wave must be created to allow the generation of 15.916 μm light from a CO_2 laser. In this case, Raman scattering involves the pumping of para-hydrogen (p-H_2) gas to a virtual state with the decay to an excited rotational state, $S(0)$ at 354.33 cm^{-1}. With this quantum of energy absorbed, an initial pumping wavelength of 10.177 μm is necessary so that exactly 15.916 μm is emitted (scattered) when the $S(0)$ level is left excited.[1] In identifying proliferation risks, the question is how a Stokes wave of 15.916 μm light is obtained.

A Raman-shifting cell with hydrogen gas will have a higher fraction of p-H_2 (spins oppositely aligned) at cooler temperatures. A cell cooled with liquid nitrogen (77 K) will have more p-H_2 than if it was left at room temperature (300 K), and using liquid H_2 (20 K) would have even more. The tradeoff is that using cooler temperatures is more expensive and marginally more complex, but that a higher threshold power per pulse is necessary at higher temperatures to generate any Raman scattered light. Once the required threshold is met, light can be passed multiple times through a Raman-shifter cell to amplify the gain by stimulated emission. W. R. Trutna and R. L. Byer[2] calculated that the Raman gain coefficient α for each pass through a shifter cell of the Stokes wave

P_{s0} (amplified according to the expression $P_s = P_{s0} \exp(\alpha)$) can be expressed as

$$\alpha = \frac{4P_p G}{\lambda_p + \lambda_s} \tan^{-1}\left(\frac{L}{b}\right) \tag{A.1}$$

where P_P is the pump power, L is the length of the cell (taken to be 3.77 m in this analysis), λ_p and λ_s are the respective pump and Stokes wavelengths, and b is a confocal parameter defined by

$$b = 2\pi\omega_{p0}^2/\lambda_p \tag{A.2}$$

where ω_{p0}^2 is the minimum pump spot size at the focus (usually referred to as the beam waist). G is the Stokes plane-wave gain coefficient of the pump intensity I_p and is given by

$$G = \frac{4\lambda_s^2 \Delta N}{n_s^2 \hbar \omega_p \Delta \omega_R}\left(\frac{d\sigma}{d\Omega}\right) \tag{A.3}$$

where ΔN in the population density, n_s is the index of refraction at the Stokes wavelength λ_s, ω_p in the pump angular frequency, $\Delta\omega_R$ is the linewidth at the full width at half-maxium, and $d\sigma/d\Omega$ is the differential cross-section for Raman scattering from the $S(0)$ state of p-H_2 by CO_2 laser pump photons. The use of circularly polarized light will increase the Raman cross section by 50 percent by suppressing anti-Stokes emission.[3] A more useful expression for G that is proportional to the Stokes frequency $\omega_s \propto \lambda_s^{-1}$ is

$$G = \frac{2\omega_s \chi_R''}{n_s n_p c^2 \epsilon_0} \tag{A.4}$$

where χ_R'' is the on-resonance Raman susceptibility (related to the cross section), and n_s and n_p are the indices of refraction of the Stokes and pump frequencies ω_s and ω_p.[4]

If the mirror reflectance inside the Raman-shifting cell is R, the net gain after n transits through the cell is

$$P_{s0}/P_s = R^n \exp[\alpha(1 + R + R^2 + ...R^n)] = \exp(\alpha_n) \tag{A.5}$$

where

$$\alpha_n = n\alpha = \alpha\left(\frac{1 - R^n}{1 - R}\right) + \ln R. \tag{A.6}$$

Thus the higher R is for mirrors used in a multiple-pass cell, the higher the net gain P_{s0}/P_s will be of the emitted Stokes wave.[5]

The threshold pumping power is defined as the gain required to amplify spontaneous Stokes power to the 1-kW level,[6] and the first proliferation concern is what is required to make this possible at a temperature 300 K. Spontaneous here refers to emission due to the Heisenberg uncertainty principle, $\Delta E \Delta t \geq \frac{\hbar}{2}$. Trutna and Byer's model[7] is used to first calculate that the Raman gain required for Stokes threshold generation is $\alpha_n = 44$. Scaling the gain coefficient $G(\text{cell pressure} = 3 \text{ atm}) = 0.5 \times 10^{-3}$ cm/MW for a pump wavelength of 1.064 μm in Equation A.4 (proportional to λ_s^{-1}) to 10.6 μm[8] gives $G(3 \text{ atm}) = 3.4 \times 10^{-5}$ cm/MW. At a pumping power $P_p = 1$ MW, the power gain coefficient per pass in a Raman cell is $\alpha = 0.08$. For a 25-transit cell with 20 effective passes[9] the net gain coefficient is $\alpha_n = 1.60$/MW. The pump power to achieve a threshold ($\alpha = 44$) is then 27.5 MW or 1.9 J in 70 ns. This should be considered only an initial CO_2 laser requirement without any advanced techniques to achieve a threshold 1 kW output at 15.916 μm.

This pump power can be decreased by a factor of 1.6 from 27.5 MW if mirrors with $R = 99$

Raman-Scattering Adjustment	Reduction Factor[11]	Threshold Power (MW)
Room Temperature (300 K)	N. A.	27.5
Cool with LN_2 (77 K)	2.4	11.5
High R (99 percent) mirrors with 40 passes	1.6	17.2
Circularly Polarized Light	1.5	18.3
Total for All Applied	**5.76**	**4.7**

Table A.1: A summary of adjustments to the Raman scattering of CO_2 laser light that could reduce the threshold peak power for a pulse to produce 1 kW Raman-shifted light at 15.916 μm. The reduction factors were obtained by comparison with a Raman cell at room temperature (300 K). The does not include the use of four-wave mixing or a seed laser, where the threshold peak power would be reduced by additional factors. If either more passes were used or the Raman cell was cooled with LH_2 (20 K), the threshold power would be reduced further. (N. A. = Not Applicable)

percent are used and 40 passes (effectively 33 for $R = 100$ percent) are made through the Raman cell. Circularly polarized light will reduce the pump power by a factor of 1.5, and cooling the p-H_2 with liquid N_2 (77 K) allows for an additional reduction factor of 2.4. These three techniques reduce the pump power by a factor of 5.76, or to a moderate resultant pump power of 4.7 MW (0.3 J for a 70 ns pulse). This should be interpreted as follows: if a minimum of 4.7 MW of peak power in a pulse from a CO_2 laser is possible, at least 1 kW of Raman-shifted light is emitted. To produce a 15.916 μm pulse of at least this power, Raman scattering a CO_2 laser pulse with 1 J of energy with a pulsed duration of 200 ns would accomplish it. If the pulse durations are higher than 200 ns, the CO_2 lasers are not export controlled by the Nuclear Suppliers Group,[10] but such lasers with pulses > 200 ns will still enrich uranium by the SILEX process as long as the energy per pulse increases accordingly to keep the peak power at 4.7 MW. This is why lasers with short pulses are preferred: the peak pulse power is easier to obtain. A summary of these possible adjustments and factors by which the threshold power would be reduced are provided in Table A.1.

The use of other Raman-shifting techniques such as four-wave mixing with a 1.06 μm Nd:YAG laser[12] or a Stokes seed laser[13] would require an even smaller threshold pump power, as would cooling the p-H_2 down to 20 K with LH_2. This would have the effect of making other laser systems with less advanced designs or less burdensome combinations (power per pulse < 4.7 MW) capable for enrichment by SILEX. The question for a proliferator would be what lasers do they know about and how accessible are they given their knowledge about how to control the required pump power to produce 15.916 μm photons. Of potential serious concern in the future in the use of a quantum cascade laser (see later section) at this wavelength as a seed laser, which would drastically lower the required threshold pump power and greatly increase the number and kind of lasers for possible SILEX use, as well as the number of potential scientists and engineers who could be enlisted in the effort. A seed laser would be capable of easy power amplification, as its initial power in a Raman cell would be much greater than that from only spontaneous emission.

Transversely Excited Atmospheric (TEA) CO_2 Laser

Transversely-Excited Atmospheric (TEA) lasers at high pressures have advantages over other systems because they are continuously tunable over a wide range of wavelengths and have very fast rise and fall times that give pulses of short duration. High pressures also make high power possible,

but what is important is the peak pulse power for reaching the required Raman threshold, not the average power over a longer time interval. It is this feature which seems to be the dominant advantage over other lasers, as one of the problems discussed with TEA CO_2 lasers is that the pulse repetition rate is low (about 1 kHz in commercially available lasers, but reported as high as 2 kHz),[14] which leaves a high fraction of UF_6 in the feed stream unirradiated. Other lasers have much higher repetition rates, but lack the capability to reach the peak power required for Raman scattering. In addition, while low repetition rates are an issue if desiring to keep capital costs low in a commercialization project, it is not a significant technical challenge for a proliferator willing to tolerate higher costs to interleave pulses from multiple lasers to increase the repetition rate. Numerous techniques are available to interleave pulses from multiple lasers,[15] as well as newly developed techniques utilizing one laser with interleaver chips to multiply the repetition rate by several factors.[16]

The high running pressures ($\sim 5-8$ atm), however, come with perhaps the greatest technical challenge in SILEX operation, which is managing the stability of the high pressure gas as it is being pulsed at high frequencies.[17] The design and manufacture of a pressure vessel requires special codes, very high electrical voltages are needed for the discharge to be triggered (~ 10 kV/cm electrode gap per atmospheric pressure), the laser gas mixture must be transported through the cavity for high repetition frequencies, and the peak energies inside the laser cavity make the lifetime of the partial reflector relatively short.[18] Such challenges seem to the author more of a technical obstacle than tuning or line-narrowing the beam, which should be possible by anyone skilled with lasers and the knowledge of diffraction gratings, etalons, piezo-electric mirrors, and many other widely published and documented techniques. Some of these techniques must be used to obtain the precise wavelength before Raman scattering, as the output from a high-pressure TEA laser likely needs tuning from its emitted wavelength.[19] High pressures make this process easier due to the overlap of the pressure-broadened transitions over four ranges (10P, 10R, 9P, and 9R) between $9.2-10.8$ μm.[20]

Commercially available TEA CO_2 lasers advertise pulse repetition rates of 1 kHz, but they can be designed and sold commercially at higher ones. Such lasers also advertise a very stable resonator cavity that does not require any adjustment after the initial alignment, lessening the most challenging technical burden in the opinion of the author. For one commercially available TEA CO_2 laser with a $1-2$ kHz repetition rate, the author has been quoted a price by a supplier between \$200,000$-$\$250,000. For 500 Hz repetition rate laser, the price would still likely exceed \$100,000. These lasers also have pulse energies and durations that exceed the threshold pump power for Raman scattering, assuming that widely reported and accessible techniques are applied.

If 2 kHz repetition rates are possible, assuming the highest performance in the public domain claimed in 1991,[21] and if the fractions of $^{235}UF_6$ already dimerized along sections of an expanding free jet were not intolerably high prior to laser irradiation, three mirror bounces could increase a 2 kHz rate to 8 kHz. Adding three more lasers in a similar fashion with interleaved pulses would create a 32 kHz repetition rate, more than the 30 kHz rate needed to irradiate all uranium. Such an arrangement would likely need to involve a number of beam telescopes (two concave lenses) to maintain a desirable amount of beam collimation along the depth of one product stream in a three-up, two-down cascade to 90 percent HEU (see Section C of this online supplement, Figure C.1). Yet with only three such streams, a total of 12 lasers would be required that today are commercially available. At \$250,000 per laser, the total laser price tag would be \$3,000,000. If it was tolerable to use twice as much time to cascade to 90 percent HEU, only 6 such lasers would be needed to acquire the same material. If dimer formation was too high in certain irradiated areas of the free jet, more lasers could be added, or perhaps a nozzle with a longer neck could be designed

to suppress dimer formation longer.

There exist many websites that describe in great detail how to build TEA lasers. This would obviously come with the challenges of managing the gas discharge, but if this is manageable, pulsing at a higher frequency to generate a repetition rate higher than 1 kHz is possible. It appears that around $\sim$ 2 kHz appears to be the optimum rate to balance capital and operating costs,[22] but more advanced technical skills could design higher performing lasers than what is commercially available, and there is information online that discusses the engineering. The challenges of high pressure gas management may even be lessened by using different isotopic mixtures of CO_2 so that the laser remains highly tunable at lower pressures.[23] If the main technical challenge is managing the high pressure gas, such a technique may be worth utilizing even if it requires more lasers to reach the desired performance characteristics. The risk with this technology it that there appear to be lots of options that a determined proliferator with advanced technical skills could choose for indigenous laser construction.

There are a number of applications with TEA lasers that may complicate identifying enrichment activities. These applications include non-destructive testing (NDT) of materials, light detection and ranging (LIDAR), differential absorption and ranging LIDAR (DIAL) to measure the concentration of gases, extreme ultraviolet (EUV) generation, many kinds of laser marking (a broad category that includes laser engraving), pulse amplification, high energy physics, and pump sources for spectroscopy.[24] These applications not only complicate identifying the intended purpose of a purchaser, but they allow knowledge about the workings of TEA lasers to spread at a rate that is proportional to the number of different applications and the scale of their use.

Other Pulsed CO_2 Lasers

There are other CO_2 lasers that pose proliferation risks, as their performance capabilities make enrichment by the SILEX process possible. These lasers would still need to be Raman-shifted, however, as the output of a CO_2 laser is between $9-11$ μm.[25] An adequate rule of thumb provided in the section above on Raman scattering is that CO_2 laser pulses need to reach a power threshold of 4.7 MW (assuming LN_2 cooling to 77 K , circular polarization, 3 atm cell pressure, and mirrors of 99 percent reflectivity) to obtain peak pulse powers of 1 kW for Raman-shifted light. This is more easily accomplished with shorter pulses, and advancements and techniques that do shorten pulse times if applied to CO_2 lasers should be monitored. However, what ultimately matters is whether 4.7 MW is attainable and if a proliferator will tolerate combinations of currently available lasers to attain this threshold.

There exist today commercially available sealed, CO_2 lasers that do not require the external gas flow of TEA lasers. There is also no challenging management of high-pressure gas. These lasers are available at around 10.2 μm, and could be tuneable to 10.177 μm at the operating pressures of 150 torr using techniques known by many scientists who work with lasers. Line narrowing the output to the desired bandwidth should be possible for those familiar with lasers as well. These lasers can emit greater than 750 W of average power at a range of repetition rates up to 200 kHz using a pulsed RF discharge with pulse durations between 2 and 1000 μs. It would still take a large number of lasers to reach 4.7 MW threshold power per pulse at a 10 kHz repetition rate, but suppose the threshold power was decreased to 2 MW with more cooling, four-wave mixing, or a seed laser (possibly a QCL at 15.91μm). Under this threshold, if lasers were ever developed that produced 4.5 kW of average power with pulse durations of 50 ns at a 10 kHz repetition rate, only

about 9 of these lasers would be needed to produce in excess of a SQ of 90 percent HEU in one year in a clandestine facility as described in Figure 3 of the paper's main section.[26] This is only $\sim$ 6 times the power output of commercially available lasers now. If pulse durations were shortened by a factor of 40 from 2 μs to 50 ns, then 54 lasers would be needed in a clandestine facility if each emitted 750 W. The author is unaware of the performance limits that physical constraints place on these systems, but the potential for future developments in this area would require only the technical expertise of someone skilled with lasers for help in using the SILEX process. Currently, unless a proliferator wishes to use hundreds of commercially available low-pressure gas lasers, a scientist skilled in the use of managing high gas pressures would be useful to increase the pulse peak power closer to the 4.7 MW threshold.

There are numerous applications for these commercially available lasers, but if the pulse durations are longer than 200 ns, they are not export controlled. In the opinion of the author, this should be changed. If a laser had 1.5 kW of average power with a 1 kHz repetition rate and pulses of 200 ns in duration, its uranium enrichment capabilities would exceed that of all commercially available TEA CO_2 lasers. The author is not aware of such a laser, but is also unaware of what limitations exist in such a system being constructed with low pressure gases $(100-150$ torr). This is only a factor of 2 higher in average power and a factor of 10 shorter in pulse duration than what can be purchased today. It remains important to be aware that combining the powers of multiple laser beams is possible and should be considered accessible by anyone skilled in working with lasers and optics.[27] The risk that a proliferator may attempt such techniques with numerous lasers depends upon the tolerance of the proliferator. What is required is determination to be successful, not sophisticated technical training measured by the types of academic degrees conferred upon the proliferators or a similar assessment of the country they are from.

Carbon Monoxide (CO) Laser at 5.3 μm

There are suggestions that a carbon monoxide (CO) laser should replace the CO_2 Raman-shifted system.[28] The advantages of this choice include the capability of irradiating all UF_6 in a cross-axial free jet[29] and a 1.8 cm^{-1} isotope shift with the $3\nu_3$ vibrational band that is three times greater than that from the ν_3 transition. This could allow for higher selectivity depending upon the narrowing of the ν_3 absorption bands or the laser linewidths of the 16 μm system. In addition, with 5.3 μm photons having three times the energy of 16 μm light, three times more collisions with ^{238} UF_6 are needed to deexcite the $3\nu_3$ mode, and this allows the CO laser to irradiate at a higher temperature ($\sim$ 150 K) where the fraction $^{235}UF_6$ monomers found in dimers is very small and more uranium is accessible per laser pulse.

The main challenge with a CO laser, however, is that the cross section for $3\nu_3$ excitation is $\sim 10^{-22}$ cm^2, or roughly $5,000-10,000$ times smaller than for the ν_3 mode. This requires that this many more photons be available per unit area, or in each pulse if its duration is short.[30] There are reportedly two ways to improve this small cross section: a continuous-wave (CW) CO laser and a mode-locked CO laser that uses a RF discharge in a supersonic stream. Both employ intracavity laser irradiation to more efficiently use energy and thereby compensate for the small $3\nu_3$ cross section. Both systems will use a very long separation unit length $(14-15$ m)[31] to limit the disadvantage from the small cross section (the author suggested 10 m with the 16 μm system), and bidirectional mirrors to redirect light back and forth for multiple passes with additional stimulated emission and amplification from the CO medium. This is not possible with the 16 μm system due to the Raman cell. In addition, the CO laser light is supposedly easier to keep collimated over long

distances with the creation of Bessel waves from large radius end mirrors in the laser cavity.[32] This is more challenging with 16 μm light due to the diffraction-limited effects at longer wavelengths, but constraints exist at all wavelengths.

Continuous-Wave (CW) CO Laser at 5.3 μm

A continuous-wave (CW) CO laser is pumped with an electric discharge that allows for the excitation of vibrational energy levels followed by their relaxation and stimulated emission of a spectrum over a broad range of wavelengths. A diffraction grating must be set at an angle to tune the laser light to a band that overlaps with the $3\nu_3$ transition of UF_6, and resonator mirrors with very high reflectivity must be used to limit cavity losses. For a cavity 15 m in length, a commercially available CW CO laser emitting 100 W of power would provide 66 kW/cm^2 when adding together the multiple passes for a free jet through a 1-cm beam diameter.[33] It is claimed that such lasers tuned to a single line (5.3 μm) can deliver 3 to 10 kW/cm^2.[34] The challenge with this design is the potential losses on the mirrors and diffraction grating, but these are skills most scientists knowledgable about lasers have or at least understand conceptually and could acquire. The efficiency is certainly limited by the need to operate on a single wavelength, so competing economically with the 16 μm system seems challenging. This depends upon the electro-optical efficiency and design of the Raman-shifting system (between 8 percent$-$14 percent total efficiency by the author's calculation), but single wavelength operation with a CW CO laser should not expect an efficiency of more than a few percent.[35]

The most important concern regarding proliferation, however, is whether this system is accessible to a proliferator and not whether it can be operated at a lower cost. The design does seem simpler than the 16 μm system (fewer components), and the electronics controlling the system are almost certainly simpler because the pressure of the gas mixture is low compared to a TEA CO_2 laser and there is no pulsed RF discharge or Q-switching. There may be more advanced tuning required with mirrors in the CW CO system, but this system seems to require fewer advanced skills and less sophisticated technical knowledge given that a Raman-shifting system is the equivalent of an additional laser. Knowing that these systems were sold to Iran in the 1970's to help with laser enrichment,[36] they should be considered a proliferation risk. In addition, CW CO lasers are not listed on the Nuclear Suppliers Group list of controlled equipment. Only CO lasers with repetition rates greater than 250 Hz appear.[37] Broad spectrum CW lasers that are commercially available for around \$100,000[38] do have to be tuned to a single wavelength, but given the widespread knowledge about how to do this, this omission appears to be a serious oversight.

Pulsed CO Laser at 5.3 μm

There is a suggestion that a pulsed CO laser could perform more efficiently than both the 16 μm Raman-shifted and a CW CO lasers.[39] Such a system would easily irradiate all uranium at a 10 MHz repetition rate, and would use a pulsed electric discharge designed to use energy as efficiently as a free-running CW CO laser that emits light within an interval of $\sim$ 4.9-6 μm. With the separation unit located between two bidirectional mirrors, 10 MHz pulses are continually propagating in both directions through the free jet containing UF_6. For light traveling at 3×10^8 m/s in a cavity 15 m long, each pulse will pass the same location along the separation unit on average every 5×10^{-8} s. For UF_6 traveling at 3×10^4 cm/s, $\sim$ 110K pulses will irradiate all UF_6 molecules traveling through a 1 cm laser diameter. For a beam with 3 kW of average power with 3 ns pulses,

this is 33 J of energy available to excite the $3\nu_3$ mode. Compared to the ~ 10 mJ required for the ν_3 mode, this 3300 factor increase is close to the $\sim 5,000-10,000$ times greater ν_3 cross section. If the average laser power is as high as 10 kW, the amount of energy available is a factor of 11,000 times greater.

This laser works by applying a RF discharge to a supersonic cross-axially flowing $CO:N_2$ medium to pump CO molecules up to a laser level that corresponds to 5.3 μm. This requires timing the pulses to allow sufficient filling of this level and a laser cavity that selects this frequency. The duration of the RF pulse discharge must be short compared to the VV-exchange to the desired level, about 10^{-7} seconds. The pulse must also be long compared to the energy exchanges between rotational levels to allow for the entire rotational level population to contribute to laser action on the desired transition.[40] About 60 W/cm^3 is the optimum power input for the $CO:N_2$ medium to allow VV-exchange from V=9 to the V=10 level and then emission on the vibrational-rotation transition of 10-9(7) corresponding to 5.3 μm light.[41] This translates into a pulse repetition rate of 10 MHz and a laser electro-optical efficiency of ~ 20 percent. The laser is mode-locked on 5.3μm with the use of an acousto-optical modulator inside the laser cavity.

The exact frequency corresponding to the $3\nu_3$ band of $^{235}UF_6$ can be fine-tuned by a number of techniques including piezo-driven micro vibrations of resonator mirrors, diffraction gratings, etalons, and others. Any broadening of the linewidth from the optical power can be adjusted with line narrowing techniques, which also include the use of etalons and diffraction gratings. There are CO transitions that allow access to $3\nu_3$ lines of $^{235}UF_6$, and the large isotope shift of 1.8 cm^{-1} should allow for some uranium enrichment even if the output wavelength is not an exact match. Whether this issue would prevent the CO laser from attaining a better energy efficiency than a Raman-shifted system is unclear to the author. However, all these listed techniques are accessible to those skilled with lasers, so this should be considered another pathway to weapons material production. Additional photon efficiency is gained by using a separation unit ~ 14 m long and a gas pressure of 1 torr at the location of laser irradiation. The gas pressure at the irradiation zone for 16 μm light is ~ 0.02 torr.[42] The means more UF_6 can be irradiated for every CO laser pulse.

A further risk with this technology is the large number of industrial applications that make identifying activities intended for uranium enrichment difficult. High-power CO lasers can be used in the the following applications: glass or ceramic cutting and welding, metal processing, surgical tissue cutting or skin resurfacing, laser sintering, and drilling multilayer boards (MLBs) and high-density interconnect structures (HDISs) for smartphones and tablets. In addition, the low absorption of 5 μm light in chalcogenide fibers opens up the possibility for delivering laser light by fiber, which is important in telecommunications technology. It should be anticipated that the number and scale of CO laser applications will grow in the future, further complicating the identification of enrichment activities.

Which laser system will ultimately prove the most economical for SILEX is uncertain. The unfortunate news is that these two systems provide routes to highly-enriched uranium that are accessible by a larger (and growing) number of scientists than if only one laser system could be utilized.

Quantum Cascade Laser at 16 μm

Quantum cascade lasers (QCLs) may be the laser system of most concern with regard to future

proliferation risks. These lasers are one of the most rapidly developing areas of applied physics, and lasers emitting up to 120 mW of power are now commercially available at wavelengths as long as 9.55 μm with very narrow linewidiths. These solid-state devices use thin materials of varying material composition to form a superlattice, where electrons can tunnel down a "cascade" of energy bands emitting one photon for each period of the superlattice. This results in a quantum efficiency greater than 1, and allows for a higher power output than semiconductor laser diodes. Power outputs of 10 W have been reported at an emitted wavelength of 4.73 μm.[43]

It has been reported in one paper on the use of QCLs for uranium enrichment measurements that the International Atomic Energy Agency (IAEA) may be trying to replace costly and time-consuming environmental sampling with laser absorption spectroscopy (LAS).[44] Environmental sampling is able to detect whether uranium is being enriched in a facility beyond declared levels, and its effectiveness is limited by how quickly samples can be analyzed and conclusions reached. The idea with LAS is that the difference between the laser power emitted from that transmitted through an air sample would be proportional to the concentration of $^{235}UF_6$ in a facility under inspection. It appears that commercial QCL technology favors the ~ 8 μm wavelength (1291 cm^{-1}) at the mid-IR combination band $\nu_1 + \nu_3$, but that future innovations will make accessible the more isolated 16 μm band (ν_3).[45] This is the band excited for SILEX with the CO_2 Raman-shifted system, and LAS safeguarding techniques will not work at this wavelength with QCLs unless scientists develop the means to access it. The laser power will likely remain low, but combing the power of multiple lasers should not be considered a significant technical barrier, even for someone without sophisticated technical training. The author is uncertain about what physical constraints exist on the power output in engineering the material of the superlattice needed for 16 μm emission, but further development of this technology should be reconsidered with respect to the proliferation risks it may create.

Section B: Dimer Formation, Nucleation, and Particle Growth

The first experimental evidence that lasers could suppress dimer formation was published by H. VandenBergh in 1985, and described the irradiation of supersonically expanded free jets of SF_6/Ar mixtures with CO_2 laser photons and the enrichments in SF_6 isotopes that were observed in the rims of free jets.[46] The result was surprising because it confirmed that dimerization occurred more quickly than previously thought possible, and could only be explained if it was dominated by low-velocity, two-body collisions. The conventional theory requiring that three-body collisions were necessary for dimer formation was updated,[47] and is in agreement with observations. The updated model allowed for the conversion of translational kinetic energy of one colliding atom or molecule to the internal vibrational or rotational energy of the other molecule absorbing the collision. In the case of forming a UF_6:G dimer, the initial kinetic energy of G must be on the order of the energy of an excited vibrational mode of UF_6. This is only possible for slow-moving molecules, and makes dimer formation more likely at low temperatures.[48]

Laser suppression of dimer formation also aids in another process that increases the enrichment of $^{235}UF_6$ in the product stream. As $^{235}UF_6^*$ forms dimers with G that quickly dissociate, unexcited $^{238}UF_6$ forms heavy dimers ($^{238}UF_6$:G or $^{238}UF_6$:UF_6) that do not. This means that $^{235}UF_6$ differs in mass by $\Delta M = M_G + 3$, where M_G is the mass of the carrier gas, from $^{238}UF_6$:G or by $\Delta M = 355$ from $^{238}UF_6$:UF_6 and will have much larger rates of escape from the free-jet core due to the radial pressure gradient, as the escape rates are proportional to ΔM. This effect was first

disclosed in Becker's studies mentioned in the introduction[49] and confirmed and further elucidated by A. A. Bochkarev, et al. with supersonic jets of argon and helium mixtures in 1970.[50] The acquired translational recoil energy in the dissociation of a $^{235}UF_6$ dimer only adds to this escape rate.

The choice of a carrier gas G to mix with UF_6 is determined by a number of competing factors. As just mentioned, the rate of radial escape due to the pressure gradient is proportional to ΔM, so a heavier carrier gas G will allow for higher separation. Upon the dissociation of $^{235}UF_6^*$:G, a heavier G will also result in $^{235}UF_6$ acquiring more translational recoil velocity from the conservation of momentum and increase separation. Choosing a carrier gas G with its own vibrational mode, however, would allow some conversion into vibrational instead of translational energy and lower the separation with slower rates of escape. A heavier carrier gas G will also not form dimers as easily since the larger kinetic energy of G will need to be absorbed by vibrational or rotational modes of the UF_6 molecule. The most important constraint is that a carrier gas G is chosen whose gas constant $\gamma = c_p/c_v$ is not too low to allow acceptable adiabatic cooling. Equation 9 of the main section of the paper provides the relationship that determines what the temperature T will be at some position downstream of the nozzle, and G must be chosen so that there is adequate cooling to separate the absorption bands of the UF_6 isotopes for high selectivity of $^{235}UF_6$. Monatomic gasses with $\gamma = 1.67$ such as Xe and Ar both appear suitable, as does SF_6 ($\gamma \approx 1.3$). If vibrational to vibrational transfers between the ν_3 mode of UF_6 (628 cm^{-1}) and the ν_4 mode of SF_6 (616 cm^{-1}) are a minor factor, SF_6 may be provide the highest enrichments and be the preferred choice.[51]

Successful condensation repression depends upon the free jet remaining in the vapor phase so that $^{235}UF_6$ molecules may migrate out of the jet core for collection by the skimmer. The necessity of forming dimers is in tension here, as dimer formation is the first step in condensation. As the UF_6/G gas is cooled by nozzle expansion, it will remain in the vapor phase well above the equilibrium vapor pressure $p_e(T)$ for some time due to the high curvature of small, spherical droplets (Kelvin effect) and the reduced binding energy per monomer of small particle clusters.[52] As dimers, trimers, and other oligomers form, a "critical embryo" size is reached after which irreversible particle growth is possible. At a pressure $p_d(T)$ well above $p_e(T)$, these "critical embryos" will irreversibly grow ("nucleation") by sweeping to their surface the condensable supply of UF_6.[53] The time required for 20 percent of the UF_6 to reach "critical embryo" size is t_c, and this must be longer than the transit time t_{tr} to collection.[54] Beyond this time t_c, significant cluster growth will impede the migration of $^{235}UF_6$ to the rim and adversely affect the enrichment factor.

Section C: Cascading to 90 Percent Highly Enriched Uranium

The arrangement of multiple separation units in a cascade for the purpose of manufacturing 90 percent HEU with third generation enrichment technology is more complex than that used for centrifuges. Constructing a cascade for centrifuges has the design advantage in that product and tails streams are sent forward and back by only one stage for further processing. Such a cascade is called 'symmetric', and the cut θ in such an arrangement will be slightly under one-half.[55] Third generation enrichment systems, however, use a smaller θ and therefore 'asymmetrical' amounts of enrichment and depletion in the two output streams. This requires that these streams be sent different numbers of stages forward or backward making the cascade design more complex. Such a design that minimizes the ratio of separative work to product produced is called 'ideal', and thereby ensures that streams of different isotopic concentrations are never mixed.

This section will consider an ideal asymmetric cascade for the manufacture of 90 percent HEU using the performance characteristics of third generation enrichment technology. The most ideal cascade, however, is not necessarily that which uses the lowest amount of separative work and may differ from what is presented here. The reason is that separative work is closely related to the rate of material flow through a separation element and is a good measure of the energy consumption of an enrichment plant only if the two can be related to each another. The is not the case with laser isotope separation. The electricity consumed depends on the minimum number of photons needed to excite the ^{235}UF$_6$ in the feed, and thus does not depend on the rate of material flow but instead on the concentration of ^{235}UF$_6$ in the flow. This explains the interest that Global Laser Enrichment (GLE) has in obtaining access to the tailings of the gaseous diffusion processes from the plant in Paducah, Kentucky, for enrichment with SILEX.[56] The energy expended in further stripping of existing tails stockpiles will be of little penalty compared to using natural uranium as feedstock.[57] For the purposes of future proliferation assessments of SILEX technology or of other laser isotope separation techniques, the "ideal" cascade will balance the capital costs (believed to be laser-dominated) against power costs for the amount of enriched product.

An Ideal Three-up, Two-down Asymmetric Cascade

As mentioned earlier, the cascade presented here considers 'ideal' to be a design that minimizes the ratio of separative work to product produced. This requires that streams of different concentrations not be mixed so that separative work is conserved, but some mixing may eventually prove more ideal in laser isotope separation processes as the power consumed is proportional to the ^{235}UF$_6$ concentration in the feed, or more accurately, the fraction of ^{235}UF$_6$ in the flow intended for excitation. The no-mixing rule applied while cascading to 90 percent HEU requires a different arrangement of process streams due to the small asymmetric cut of $\theta = 0.25$ at favorable running conditions. If θ is $1/n$, in general this means that there will be $n-1$ parallel product streams where the product streams from each stage are sent forwards $n-1$ stages.[58] Waste streams could be sent back either one or two stages, but two allows for more flexibility with the geometrical arrangements of parts within separation units and was chosen here for that reason. This is referred to as a three-up, two down asymmetric cascade (three product streams and two waste streams) and is shown in Figure C.1.

The general method for calculating the flows and concentration of an ideal cascade with asymmetrical units was provided by D. Wolf et al. in 1976[59] and was followed in constructing this cascade. The crucial assumption in this method is that all stages have the same separation factor α. The estimated optimal running parameters have suggested an enrichment factor of 2 with a cut of 0.25 for each separation unit, but the condition of no mixing in this cascade means that the enrichment factor for each stage β_{stage}, as opposed to each separation unit, can be found from the expression

$$\beta_{\text{stage}} = \alpha^{1/(k+l)} \tag{C.1}$$

where the separation factor $\alpha = 3$ for each stage and k is the number of stages the product stream must pass forward before entering the next separation step and l is the number of stages the waste stream must move back. For this three up, two-down cascade, $k = 3$, $l = 2$, and $\beta_{\text{stage}} = 1.2457$. Two cascades were simulated in this analysis: one with only natural uranium feedstock (uranium-235 concentration = 0.7 percent) and the other with reactor-grade uranium feedstock (uranium-235 concentration = 3.5 percent). The cascade with natural uranium may be a more relevant concern with regard to third generation laser enrichment technology, as it is the most likely feedstock for a clandestine facility. The challenges of material accountancy with safeguards at declared facilities
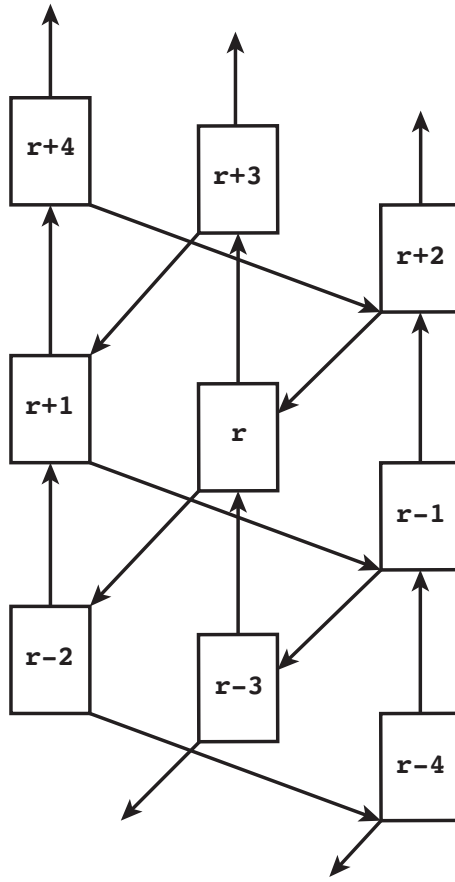
Figure C.1: A section of a three-up, two-down asymmetric cascade

are certainly real, however, and the undetected diversion of reactor-grade uranium for further enrichment in a clandestine facility must still be considered. The feed concentration for these cascades was thus either $N_F = 0.035$ or $N_F = 0.007$, the desired HEU concentration in the final product $N_P = 0.90$, and the final tails concentration was $N_T = 0.002$ for the $N_F = 0.035$ cascade and $N_T = 0.001$ for the $N_F = 0.007$ one. There is nothing significant about choosing different tails concentrations between the cascades, as both are certainly possibilities. Choosing a lower concentration in tails could be selected if a more efficient use of the initial uranium feedstock is desired at the expense of requiring a larger space for more separation units. As previously mentioned, laser isotope separation facilities require smaller energy costs with the enriching of more depleted tails since the energy required is not strictly tied to the flow rate through the separation units.

The concentration profile along each stage in the cascades was calculated by starting with the relative isotopic abundance in the feed at some stage r, R_{F_r}, and multiplying it by β_{stage} at each stage until the desired product concentration $N_P = 0.9$ was reached. The number of times this needed to be done was equal to the number of enriching stages in the cascade. The number of stripping stages was obtained by how many times R_F was divided by β_{stage} to reach $N_T = 0.002$ or 0.001. To be accurate, the number of stripping stages was this number minus one, as the stage with the initial feedstock was counted as an enrichment stage. The relevant parameters and expressions used in determining the concentration profile of the cascades are listed in Table C.1.

The cascade's flow profile was calculated by first writing down the material balance equation

Uranium Feedstock Concentration	$N_F = 0.035$	$N_P = 0.007$
For each stage: $\alpha^{1/(k+l)} = \beta_{\text{stage}}$	1.2457	1.2457
For any enriching stage r: $\mathbf{R_{F_{r+1}}} = \mathbf{R_{F_r}} \cdot \beta_{\text{stage}}$		
Number of enriching stages	25	32
For any stripping stage r: $\mathbf{R_{F_{r-1}}} = \mathbf{R_{F_r}} \cdot \beta_{\text{stage}}^{-1}$		
Number of stripping stages	12	7
Total number of stages in cascade	37	39

Table C.1: The parameters and expressions used for determining the concentration profile of the asymmetric cascades with either 3.5 percent enriched or natural uranium (0.7 percent) feedstock.

for the flow into and out of stage r:

$$W_{r+l} + P_{r-k} = F_r = W_r + P_r \tag{C.2}$$

and the isotope material balance for stage r:

$$W_{r+l} \cdot N_{W_{r+l}} + P_{r-k} \cdot N_{P_{r-k}} = F_r \cdot N_{F_r} = W_r \cdot N_{W_r} + P_r \cdot N_{P_r} \tag{C.3}$$

If follows from the condition of no mixing that the following cascade streams must have the same concentration of $^{235}\text{UF}_6$:

$$N_{W_{r+l}} = N_{P_{r-k}} = N_{F_r} \tag{C.4}$$

Equation C.3 can then be rewritten as

$$F_r N_{F_r} = (F_r - P_r)N_{W_r} + P_r N_{P_r} \tag{C.5}$$

which can rearranged to give the cut

$$\theta_r = \frac{P_r}{F_r} = (N_{F_r} - N_{W_r})/(N_{P_r} - N_{W_r}) \tag{C.6}$$

Since θ_r is a function of concentration only, it can be calculated for each stage once the concentrations are calculated.

Since it is unknown what the ratios are between the various product and waste streams, Wolf et al. proposed a solution that started with the material balance of feed to each stage:

$$F_r = W_{r+l} + P_{r-k} + F \tag{C.7}$$

where F is the external stream to or from the stage. It is zero except when feed is added to or side products are extracted from the cascade. This equation can be expressed in terms of the cut as

$$F_r = (1 - \theta_{r+l}) \cdot F_{r+l} + \theta_{r-k} \cdot F_{r-k} + F \tag{C.8}$$

which provides a set of linear equations that include every stage of the cascade. The external feed F and θ_r are known for every stage, and the goal is to solve for the feed flow rates F_r to calculate the cascade's entire flow profile. The matrix form of Equation C.8 is

$$\mathbf{F_r} = \theta \mathbf{F_r} + \mathbf{F} \tag{C.9}$$

which can be rearranged to solve for $\mathbf{F_r}$ as

$$\mathbf{F_r} = (\mathbf{I} - \theta)^{-1}\mathbf{F} \qquad (C.10)$$

Finding the inverse of the matrix $\mathbf{I} - \theta$ and knowing the external feed F at each stage allows for calculation of F_r at each stage r.

For $N_F = 0.007$, the flow rate was calculated with the only external feed being 5000 kg of natural uranium (0.7 percent) into stage 8. The heads flow in stages 37, 38, and 39 are collected as product, and the tails flow in stages 1 and 2 are discarded as the final depleted streams. The yearly production from this cascade is 32.5 kg of HEU enriched to 90.3 percent, which equals 153.8 kg of natural uranium needed for every kilogram of weapon-grade material produced. The total required separation unit length (nozzle depth) is 35.25 m, and has lengths for each stage that are scaled to the flow through one meter, 1933.4 kg/yr.

For $N_F = 0.035$, the flow rates F_r for each stage were calculated with the only external feed F being 1000 kg of 3.5 percent enriched uranium into stage 13. The three product stages are 35, 36, and 37, the two waste streams are 1 and 2, and the flows for each stream are in kg of uranium/year. The average concentration of uranium-235 in the product streams is near 90 percent, making the total heads flow equal to the amount of HEU produced. The yearly production is 36.4 kg of HEU enriched to 91.2 percent with an external feed rate of only 1000 kg of 3.5 percent uranium/year. This requires only 27.5 kg of 3.5 percent enriched feed for every kilogram of weapon-grade material. The required separation unit length is 11.37 m.

The uranium resource requirements and total separation unit length for both cascades are displayed in Table 2 of the main section of the paper.

Section D: Model of Enrichment Factor β

This appendix confirms that the author's calculated minimum laser performance requirements allow for the use of $\beta \sim 2$ and other optimal running parameters (Table 1 of the paper's main section) as provided in J. Eerkens analysis.[60] It has two other purposes, however: It simplifies Eerkens' expression for β, which is necessary for estimates at higher enrichment levels, and it discusses how the steady-state assumptions in Eerkens' model do not accurately model the evolution of a free jet. The consequences of this steady-state assumption may significantly underestimate the maximum value of $\beta \sim 2$, which would decrease both the required space for a clandestine third generation laser enrichment plant and the energy consumption per separative work unit.

A Model of β for Third Generation Laser Enrichment Technology

An important characteristic of any enrichment technology is the size of its enrichment factor β, a measure of the change in relative abundance of uranium-235 to uranium-238 from the feed to the product stream. Restating Equation 1, β can be expressed as

$$\beta = \frac{N_P/(1 - N_P)}{N_F/(1 - N_F)} = \frac{R_P}{R_F} \qquad (D.1)$$

where N_P and N_F are the respective concentrations of $^{235}\text{UF}_6$ in the product and feed, and $R_P = N_P/(1 - N_P)$ and $R_F = N_F/(1 - N_F)$ are the respective relative isotopic abundances of

^{235}UF$_6$ to ^{238}UF$_6$ in those streams. What follows is a model for calculating the enrichment factor β for third generation laser enrichment processes. It is heavily based on a model from the only analysis[61] that has attempted to provide explicit relations for the migration of ^{235}UF$_6$ molecules to the outskirts of a supersonic free jet based upon the dynamics of the different species within the gas.

The enrichment factor β must first be redefined to become more applicable to higher enrichment levels. What is collected by the skimmer in the product stream are ^{235}UF$_6$ and ^{238}UF$_6$ molecules that have escaped from the jet core. The enrichment factor β can then be defined as

$$\beta = \frac{x'_{235}/(1 - x'_{235})}{x_{235}/(1 - x_{235})} \tag{D.2}$$

where x'_{235} is the concentration of ^{235}UF$_6$ collected by the skimmer as product

$$x'_{235} = [\text{All escaped } ^{235}\text{UF}_6] \div [\text{All escaped UF}_6] \tag{D.3}$$

and x_{235} is the concentration of ^{235}UF$_6$ in the feed.

What must first be established is the different species that exist in the free jet. All ^{235}UF$_6$ molecules are distributed across four different forms: ^{235}UF$_6$:G dimers, laser-excited ^{235}UF$_6^*$ monomers, unexcited ^{235}UF$_6$ monomers, and ^{235}UF$_6^!$ epithermals. The ^{235}UF$_6^!$ molecules are produced upon the rapid dissociation of ^{235}UF$_6^*$:G dimers, where the vibrational energy of ^{235}UF$_6^*$ is converted to translational recoil energy at above-thermal, or "epi-thermal", velocities that allow for faster migration than unexcited ^{235}UF$_6$. All ^{238}UF$_6$ molecules exist in one of two forms: either non-excited ^{238}UF$_6$ monomers or ^{238}UF$_6$:G dimers. All of these six types, with the exception of ^{235}UF$_6^*$ and ^{235}UF$_6$, will migrate away from the jet core at different rates due to different collisional cross-sections and average molecular speeds. When considering a material balance for all of these types,

$$f^*_{235} + f_{235} + f^!_{235} + f^d_{235} = 1 \qquad \text{and} \qquad f_{238} + f^d_{238} = 1 \tag{D.4}$$

where f^*_{235}, f_{235}, $f^!_{235}$, and f^d_{235} are the respective steady-state fractions of ^{235}UF$_6^*$, ^{235}UF$_6$, ^{235}UF$_6^!$, and ^{235}UF$_6$:G in all forms of ^{235}UF$_6$, and f_{238} and f^d_{238} are the respective steady-state fractions of ^{238}UF$_6$ and ^{238}UF$_6$:G in all forms of ^{238}UF$_6$.

Each of these species will have different escape fractions Θ to the rim of the gas for collection as product due to the different migration rates away from the jet core. This allows Equation D.3 to be rewritten as

$$\begin{aligned}
x'_{235} &= [\text{All escaped } ^{235}\text{UF}_6] \div [\text{All escaped UF}_6] \\
&= [x_{235}\{(1 - f^!_{235} - f^d_{235})\Theta^m + f^!_{235}\Theta^! + f^d_{235}\Theta^d\}] \\
&\quad \div [(1 - x_{235})\{(1 - f^d_{238})\Theta^m + f^d_{238}\Theta^d\} \\
&\quad + x_{235}\{(1 - f^!_{235} - f^d_{235})\Theta^m + f^!_{235}\Theta^! + f^d_{235}\Theta^d\}]
\end{aligned} \tag{D.5}$$

where Θ^m, $\Theta^!$, and Θ^d are the respective escape fractions for UF$_6$ thermal monomers, epithermals, and dimers. These different escape fractions are due to the different migration rates out of the jet core for these three groups, and the different rates due to the slightly different masses of ^{235}UF$_6$ and ^{238}UF$_6$ thermal monomers are ignored, as they are small compared to these other group differences.

With a relationship between x'_{235} and the fractions and migration rates of different groups in the jet, β can now be expressed as

$$\beta = \frac{(1 - f^!_{235} - f^d_{235})\Theta^m + f^!_{235}\Theta^! + f^d_{235}\Theta^d}{(1 - f^d_{238})\Theta^m + f^d_{238}\Theta^d} \tag{D.6}$$

SILEX Running Parameter	J. W. Eerkens[65]	R. Snyder
Pressure of SF_6 (torr) at location of laser irradiation	0.02	0.026
Temperature (K)	35	42
Enrichment factor β	1.95	1.93
UF_6 concentration in carrier gas G	0.02	0.04
Laser power (Watts)	1000	374
Length of jet core (cm)[66]	20	20
Total Product Cut (θ)	0.25	0.25
Pressure of SF_6 (torr) at skimmer for collection	0.002	0.003

Table D.1: SILEX running parameters obtained by J. W. Eerkens (2005) and the author

which is a simpler result than what appears in the analysis[62] upon which this model is based. The original model only considered an expression for β that was a ratio of $^{235}UF_6$ concentrations, x'_{235}/x_{235}, in the collected gas rim to the feed stream. This is approximately true as long as the concentration of $^{235}UF_6$ is low, which works well for reactor-grade enrichment levels. The model that appears in Equation D.6 is true for any enrichment level, and is more accurate when cascading to higher enrichments for weapons material. It is also an important result in that it does not depend upon x_{235}.

Another important characteristic of third generation laser enrichment technology is the product cut θ, which is simply the fraction of the feed stream collected as product. It can be expressed in terms of already defined parameters as

$$\theta = x_{235}\{(1 - f^!_{235} - f^d_{235})\Theta^m + f^!_{235}\Theta^! + f^d_{235}\Theta^d\} + (1 - x_{235})\{(1 - f^d_{238})\Theta^m + f^d_{238}\Theta^d\} \qquad (D.7)$$

and must be large enough to make the process attractive economically. Low values for θ would require higher amounts of uranium feedstock or perhaps a more complicated cascade design with more separation units and a larger physical footprint. Equation D.7 shows θ to be dependent upon x_{235}, which is consistent with the size of the cut increasing with $^{235}UF_6$ concentration when cascading to weapons material.

To avoid significantly expanding the length of this paper, the detailed relationships for all symbols in Equation D.6 are exactly the same as in the 2005 paper by J. W. Eerkens[63] and are not reproduced here. The form of Equation D.6 is simple enough to accurately discuss the limitations of this model. For the purposes of justifying the assumptions made in this paper that serve as inputs into the cascade for producing weapons material, however, it is important to state that the results of the model recreated by the author largely agree with those presented in J. W. Eerkens (2005) despite the slightly different formulations.

J. W. Eerkens presents a case that reasonable parameters for the SILEX process can be chosen from Figures 5A, 5B, 9A, and 9B of the 2005 paper,[64] which display how β and θ for UF_6 mixed with possible carrier gases vary with temperature at a fixed pressure of 0.01 torr and with pressure at a fixed temperature of 35 K. SF_6 is likely the most preferred carrier gas, but Ar and Xe are other possible choices.

Results from J. W. Eerkens and the author are displayed in Table D.1. Limitations of the model in Equation D.6 are revealed here, with two different pressures for SF_6, 0.026 torr and 0.003 torr, listed by the author. J. W. Eerkens does not accurately model the parameter changes as the free jet expands in the separation unit, as the model requires a constant temperature and pressure as inputs. However, an accurate model of these parameter changes in an expanding free jet is necessary to accurately calculate β. The author chose 0.026 torr at the location of laser irradiation to provide a sufficiently high β, but 0.003 torr where product was collected at the skimmer to allow a sufficiently high θ. The concept upon which this enrichment process is based is that as many $^{235}UF_6$ monomers as possible need to be available for laser excitation, followed by the formation of the maximum number of dimers which then quickly dissociate. This can only happen at a temperature significantly higher than 42 K (Table D.1), where according to the author's version of the model 10 percent of $^{235}UF_6$ molecules already exist in dimers. If laser irradiation occurred at the more desirable temperature of 100 K, almost no $^{235}UF_6$ molecules are found in dimers. As the free jet cools from this temperature, laser-excited $^{235}UF_6^*$ will form more $^{235}UF_6^*$:G dimers than if laser excitation had occurred at 42 K. This allows the term $f_{235}^!\Theta^!$ in Equation D.6 to increase, as more epithermal molecules will be present in the jet. As the jet continues to cool and the pressure lowers, all cuts (Θ^m, $\Theta^!$, and Θ^d) will grow, and with $\Theta^! > \Theta^m > \Theta^d$ it follows that β will as well. This evolving dynamic is not accounted for in the above model and is why $\beta \approx 2$ appears to be an underestimate. If β is indeed higher, third generation laser enrichment technology will require less space and use energy more efficiently than what is estimated in the main section of this paper.

Notes for Supplementary Material

[1] It was suggested in a document after visiting a SILEX pilot plant that before Raman scattering, the CO_2 laser light was tuned to 10.8 μm before scattering off of p-H_2. At this initial wavelength, however, it would appear that scattering off of normal-deuterium (n-D_2) would be necessary to down shift to 15.916 μm. The $S(1)$ state of n-D_2 is 297.52 cm^{-1}. Given that the scientific literature provides more examples for scattering from p-H_2 than n-D_2, and knowing that n-D_2 is more expensive and difficult to acquire than p-H_2, this analysis was done under the assumption that p-H_2 was used. This would require an initial wavelength of 10.177 μm, not 10.8 μm. Available at: John L. Lyman, Enrichment separative capacity for SILEX, LA-UR-05-3786, 2005. https://www.fas.org/sgp/othergov/doe/lanl/docs4/silex.pdf

[2] W. R. Trutna and R. L. Byer, "Multiple-pass Raman gain cell," *Applied Optics* 19 (1980): 301−312.

[3] R. W. Minck, E. E. Hagenlocker, and W. G. Rado, *Phys. Rev. Lett.* 17 (1966): 229−231. A $\lambda/4$ plate or Frensel rhomb can be used to convert incident linear light from the CO_2 laser to circular light prior to entering the Raman-shifting cell.

[4] Ibid., 305.

[5] Ibid., 305.

[6] Ibid., 307.

[7] Ibid.

[8] The needed Stokes wavelength is 10.177 μm, but this is a close enough approximation to get an idea of what is possible

[9] Assumes R = 98 percent

[10] IAEA, INFCIRC/254/Rev.9/Part 2.

[11] Trutna and Byer, "Multiple-pass Raman gain cell," 310.

[12] Ibid.

[13] J. L. Carlsten and R. G. Wenzel, "Stimulated Rotational Raman Scattering in CO_2-Pumped Para-H_2," *IEEE Journal of Quantum Electronics* QE-19 (1983): 1407−1413.

[14] A commercially available system with a 1 kHz repetition rate can be found here: "TEA Series - UT", Par Systems, accessed September 15, 2015, http://www.par.com/technologies/pulsed-co2-lasers/lasers/co2-lasers/. Rates as high as 2 kHz were reported here: Kemp et al., "Uranium Enrichment Technologies in South Africa."

[15] "Time Division Multiplexing," RP Photonics Encyclopedia, https://www.rp-photonics.com/

[16] M. Sander, S. Frolov, J. Shmulovich, E. Ippen, and F. Kartner, "10 GHz femtosecond pulse interleaver in planar waveguide technology" *Optics Express* 20 (2012).

[17] Ronander et al., "High-pressure continuously tunable CO_2 lasers and molecular laser isotope separation."

[18] Ibid., 53.

[19] Lyman, "Enrichment separative capacity for SILEX."

[20] P. Repond and M. W. Sigrist, "Continuously Tunable High-Pressure CO_2 Laser for Spectroscopic Studies on Trace Gases," *IEEE Journal of Quantum Electronics* 32 (1996).

[21] Kemp et al., "Uranium Enrichment Technologies in South Africa."

[22] Ronander et al., "High-pressure continuously tunable CO_2 lasers and molecular laser isotope separation."

[23] L. R. Botha, High repetition rate continuously tunable CO2 laser system investigation (PhD diss., University of Natal, South Africa, 1990)

[24] A conversation with a commercial supplier of TEA lasers revealed that a higher standard exists for proving whether a potential purchaser's stated intention for the use of high-performance TEA lasers is true. The implication here is that if high-performance TEA lasers will not be sold unless the purchaser is well identified, it is therefore possible that lasers with more modest capabilities could be acquired from a commercial supplier despite export controls.

[25] There have been attempts to produce a 16μm laser by lasing on different bands of the CO_2 molecule by using UV preionization techniques to prepare the active medium (thereby avoiding the need to Raman shift), but the author does not know of any such commercially supplied lasers. There are some journal articles discussing the dynamics of such systems, but certainly not wide investigation.

[26] See Figure 5 in Carlsten and Wenzel, "Stimulated Rotational Raman Scattering in CO_2-Pumped Para-H_2." The equation of this line between 0.2 and 0.6 J of pump power is $0.0005(10)^{6.75x}$, where x is the pump power of the CO_2 laser after reaching the peak power threshold. With a y-intercept of 5×10^{-5} indicating the Stokes energy for a 1 kW pulse produced at threshold and a duration of 50 ns, an additional 0.35 in pump energy is necessary to crete the minimum $\sim$ 10 mJ pulse to excite all uranium by laser irradiation in SILEX.

[27] T. Y. Fan, "Laser Beam Combining for High-Power, High-Radiance Sources," *IEEE Journal of Selected Topics in Quantum Electronics* 11 (2005).

[28] Baranov and Koptev, "Mode-Locked CO Laser for Isotope Separation of Uranium Employing Condensation Repression," and I. Baranov and Andrey V. Koptev, "Pulsed CO Laser for Isotope Separation of Uranium," *AIP Conference Proceedings* 1464 (2012): 689, doi: 10.1063/1.4739921 and J. Eerkens, "Process and Apparatus for Condensation Repressing Isotope Separation by Laser Activation," U. S. Patent 270,035, filed Mar. 12, 2014, and issued Sep. 18, 2014.

[29] Baranov and Koptev, "Mode-Locked CO Laser for Isotope Separation of Uranium Employing Condensation Repression."

[30] It is important to remember here that $\sigma(3\nu_3) \propto \sqrt{T}$, so that the $5,000-10,000$ times smaller cross section compared to $\sigma(\nu_3)$ may be altered if the larger isotope shift allows for laser irradiation at a higher temperature.

[31] Baranov and Koptev, "Mode-Locked CO Laser for Isotope Separation of Uranium Employing Condensation Repression," and Baranov and Koptev, "Pulsed CO Laser for Isotope Separation of Uranium," and Eerkens, "Process and Apparatus for Condensation Repressing Isotope Separation by Laser Activation."

[32] Eerkens, "Process and Apparatus for Condensation Repressing Isotope Separation by Laser Activation."

[33] This was obtained by calculating that 2.22 J will be flowing through a free jet in the time it takes a UF_6 molecule to travel through a beam of 1-cm diameter. If it takes 3.33×10^{-5} s to travel 1 cm, the power circulating in the cavity will be $2.22/3 \times 10^{-5} = 66.667$ kW/cm^2.

[34] Eerkens, "Process and Apparatus for Condensation Repressing Isotope Separation by Laser Activation."

[35] Baranov and Koptev, "Pulsed CO Laser for Isotope Separation of Uranium."

[36] A. Khlopkov, "How the United States Helped Iran Build a Laser Enrichment Laboratory," *The Nonproliferation Review*, 20 (2013): $39-62$.

[37] IAEA, INFCIRC/254/Rev.9/Part 2.

[38] This average price was provided to the author in a conversation with a representative from a major laser supplier.

[39] IBaranov and Koptev, "Pulsed CO Laser for Isotope Separation of Uranium."

[40] The idea here is for every occupied level to populate the rotational level with the highest gain if this level is continuously emptied by stimulated emission. A long pulse ($\sim 3-10$ ns) compared to rotational transitions (1 ns) therefore allows for the most efficient use of energy if some 5.3 μm light is created that otherwise could not be with a shorter pulse.

[41] This nomenclature indicates stimulated emission from the 10th to the 9th vibrational level at a rotational level of 7.

[42] Both of these pressures at the location of irradiation assume a beam with 1 cm diameter.

[43] Yao et al., *Nanoscale Research Letters*, 10 (2015): 177.

[44] R. Lewicki et al., "Quantum cascade laser absorption spectroscopy of UF_6 at 7.74 μm for analytical uranium enrichment measurements." *Proceedings of SPIE- The International Society for Optical Engineering*, January 2010.

[45] Ibid.

[46] H. VandenBergh, "Laser Assisted Aerodynamic Isotope Separation," *Laser ind Optoelectronik* 3 (1985): 263-273.

[47] Eerkens, "Equilibrium dimer concentrations in gases and gas mixtures," 196.

[48] Ibid., 206. It is worth noting that at a temperature of $T = 300$ K, $kT = 0.025$ eV and that the kinetic energy in one degree of freedom of a gaseous species is $\frac{1}{2}kT$, where k is the Boltzmann constant.

[49] Becker, Bier, and Burghoff, "Die Trenndiise-Ein neues Element zur Gas- und Isotopen-trennung."

[50] A. A. Bochkarev et al., "Structure of a supersonic jet of an argon-helium mixture in a vacuum," *Journal of Applied Mechanics and Technical Physics* 11 (1970): 857-861.

[51] Eerkens, "Laser-induced migration and isotope separation of epi-thermal monomers and dimers in supercooled free jets," 252.

[52] J. W. Eerkens, "Nucleation and particle growth in supercooled flows of SF_6/N_2 and UF_6/N_2 mixtures," *Chemical Physics* 293 (2003): 111-153.

[53] Ibid., 112.

[54] Eerkens, "Laser-induced migration and isotope separation of epi-thermal monomers and dimers in supercooled free jets," 248

[55] A. S. Krass, P. Boskma, B. Elzen, and W. A. Smit, *Uranium Enrichment and Nuclear Weapon Proliferation*, Stockholm International Peace Research Institute (Taylor & Francis, 1983).

[56] "Laser enrichment chosen for Paducah," World Nuclear News, November 28, 2013, http://www.world-nuclear-news.org/enf-laser-enrichment-chosen-for-paducah-2811137.html.

[57] C. P. Robinson and R. J. Jensen, "Laser Methods of Uranium Isotope Separation," in *Uranium Enrichment*, ed. S. Villani (Springer-Verlag Berlin Heidelberg, 1979): 269-290.

[58] Krass, et al., *Uranium Enrichment and Nuclear Weapon Proliferation*

[59] D. Wolf, J. L. Borowitz, A. Gabor, Y. Shraga, "A General Method for the Calculation of an Ideal Cascade with Asymmetric Units," *Ind. Eng. Chem. Fundam.* 15 (1976).

[60] Eerkens, "Laser-induced migration and isotope separation of epi-thermal monomers and dimers in supercooled free jets."

[61] Ibid.

[62] Ibid., 239.

[63] Ibid.

[64] Ibid., 242-243, 248-249.

[65] Ibid.

[66] length of the free jet from nozzle to skimmer